

Smoothed Wigner functions: a tool to resolve semiclassical structures

A.M.F. Rivas^{1,2,a}, E.G. Vergini¹, and D.A. Wisniacki³

¹ Departamento de Física, Comisión Nacional de Energía Atómica. Av. del Libertador 8250, 1429 Buenos Aires, Argentina

² Instituto de Ciencias, Universidad Nacional de General Sarmiento, J.M. Gutierrez 1150,
1613 Los Polvorines Prov. Buenos Aires, Argentina

³ Departamento de Física “J.J. Giambiagi”, FCEN, UBA, Pabellón 1, Ciudad Universitaria, 1428 Buenos Aires, Argentina

Received 18 August 2004

Published online 21 December 2004 – © EDP Sciences, Società Italiana di Fisica, Springer-Verlag 2004

Abstract. The Wigner and Husimi distributions are the usual phase space representations of a quantum state. The Wigner distribution has structures of order \hbar^2 . On the other hand, the Husimi distribution is a Gaussian smearing of the Wigner function on an area of size \hbar and then, it only displays structures of size \hbar . We have developed a phase space representation which results a Gaussian smearing of the Wigner function on an area of size \hbar^σ , with $\sigma \geq 1$. Within this representation, the Husimi and Wigner functions are recovered when $\sigma = 1$ and $\sigma \gtrsim 2$ respectively. We treat the application of this intermediate representation to explore the semiclassical limit of quantum mechanics. In particular we show how this representation uncover semiclassical hyperbolic structures of chaotic eigenstates.

PACS. 05.45.Mt Quantum chaos; semiclassical methods – 03.65.Sq Semiclassical theories and applications

From the origin of quantum theory different representations of it were extensively studied in the literature. In particular, a phase space representation appears as the natural selection in the fundamental problem of the semiclassical limit of quantum mechanics [1,2]. A phase space description of quantum mechanics will indeed show most clearly classical features, as the phase space is the context where classical mechanics naturally emerges. For instance, quantum manifestations of chaos are clearly observed in the Wigner [3] or Husimi distributions [4].

Although Wigner and Husimi distributions contain all the information of a quantum state, they display different characteristics. The Wigner function shows big oscillations with negative value which distinguish it from a classical probability density. For instance, on a compact phase space of area A , it develops fine structures on a sub-Planck scale of order \hbar^2/A [5]. These sub-Planck structures are manifestations of quantum interferences from distant localized objects and enhance the sensitivity of a state to perturbations [5–7]. On the other hand, the Husimi function is a Gaussian smearing of the Wigner function on an area of size \hbar that washes out the negative part and hence it is suitable as a probability density. However, this smoothing hides important structures such as semiclassical hyperbolic structures embedded in chaotic eigenfunctions [8]. In synthesis, the Wigner func-

tion displays high resolution but it is not free of long range quantum interferences, while the Husimi function that washes out quantum interferences also hides important semiclassical structures. This implies the need for a phase space representation of quantum mechanics that is able to explore intermediate regimes. This is the case of the s -parametrized quasi-distribution originally introduced by Cahill and Glauber [9]. A tool that is widely used in optics (see for example [10]) but ignored by the semiclassical community. In this paper, we insert the s -parametrized quasi-distribution into the powerful formalism of reflection operators [15], this allows to show that intermediate smoothing of the Wigner function are good representations of quantum mechanics. We then illustrate the usefulness of this representation to resolve semiclassical structures, for this purpose we show how this smearing is relevant to describe the scarring phenomenon, one of the most important problems in quantum chaos [11,12]. The formalism is presented for the case of a plane phase space with one degree of freedom, the extension for several degrees of freedom is straightforward and the technical details regarding the topology of a cylindrical phase space will be presented elsewhere [13].

In what follows, we will work with adimensional variables p, q and \hbar . With this purpose, we measure all the physical magnitudes in units of the characteristic values of the problem [14]. Among the several representations of quantum mechanics, the Weyl-Wigner representation is

^a e-mail: rivas@tandar.cnea.gov.ar

the one that performs a decomposition of the operators that acts on the Hilbert space, on the basis formed by the set of unitary reflection operators \hat{R}_x of center point $x = (q, p)$ in phase space (see [15]). The set of reflection operators, are formally defined in [15] as the Fourier transform of the translation (or Heisenberg) operators. Their action on the coordinate and momentum bases are

$$\begin{aligned}\hat{R}_x |q_a\rangle &= e^{2i(q-q_a)p/\hbar} |2q - q_a\rangle \\ \hat{R}_x |p_a\rangle &= e^{2i(p-p_a)q/\hbar} |2p - p_a\rangle,\end{aligned}$$

displaying the interpretation of these operators as reflections in phase space.

This family of operators have the properties that they are a decomposition of the unity (completeness relation) and satisfy an orthogonality relation

$$\begin{aligned}\hat{1} &= \frac{1}{2\pi\hbar} \int dx \hat{R}_x, \\ \text{Tr} [\hat{R}_{x_1} \hat{R}_{x_2}] &= 2\pi\hbar \delta(x_2 - x_1).\end{aligned}\quad (1)$$

Hence, an operator \hat{A} can be decomposed in terms of reflection operators as follows

$$\hat{A} = \frac{1}{2\pi\hbar} \int dx A_W(x) \hat{R}_x.$$

With this decomposition, the operator \hat{A} is mapped on a function $A_W(x)$ living in phase space, the so called Weyl-Wigner symbol of the operator. Using (1) it is easy to show that $A_W(x)$ can be obtained by performing the following trace operation

$$A_W(x) = \text{Tr} [\hat{R}_x \hat{A}].$$

Of course, as it is shown in [15], the Weyl symbol also takes the usual expression in terms of matrix elements of \hat{A} in coordinate representation

$$A_W(x) = \int \left\langle q - \frac{Q}{2} \left| \hat{A} \right| q + \frac{Q}{2} \right\rangle \exp\left(-\frac{i}{\hbar} p Q\right) dQ.$$

On the other side, instead of using reflection operators, the Husimi representation is related with the expansion of operators in terms of the set of projectors on coherent states $\hat{\rho}_X = |X\rangle \langle X|$ [16,17], where $|X\rangle$ is the coherent state centered at the point $X = (Q, P)$

$$\langle q | X \rangle = \left(\frac{\omega}{\pi\hbar}\right)^{1/4} \exp\left[-\frac{\omega}{2\hbar} (q - Q)^2 - \frac{i}{\hbar} P q\right].$$

The parameter ω stands for the form factor since the dispersions $\Delta q = \sqrt{\hbar/2\omega}$ and $\Delta p = \sqrt{\hbar\omega/2}$ satisfy $\Delta p/\Delta q = \omega$, while the product $\Delta q \Delta p = \hbar/2$ displays the least uncertainty independently of ω .

As for the reflection operators, the set of projectors $\hat{\rho}_X$ also form a decomposition of the unity

$$\hat{1} = \frac{1}{2\pi\hbar} \int dX \hat{\rho}_X$$

where $dX \equiv dP dQ$. Nevertheless, they are not orthogonal since their traces satisfy (see [16])

$$\text{Tr} [\hat{\rho}_{X'} \hat{\rho}_X] = |\langle X' | X \rangle|^2 = 2\pi\hbar G_{2\hbar}(X' - X),$$

where we have used the following definition for a Gaussian distribution in phase space

$$G_\alpha(X' - X) \equiv \frac{1}{\pi\alpha} \exp\left\{-\frac{1}{\alpha} \left[\omega(Q' - Q)^2 + \frac{1}{\omega}(P' - P)^2\right]\right\}.$$

Now, by expanding \hat{A} in terms of the projectors $\hat{\rho}_X$

$$\hat{A} = \frac{1}{2\pi\hbar} \int dX \tilde{A}_H(X) \hat{\rho}_X, \quad (2)$$

the operator is mapped on the function $\tilde{A}_H(X)$, the so called contravariant symbol of the operator. Moreover, by taking the trace operation we get the covariant symbol

$$A_H(X) = \text{Tr} [|X\rangle \langle X| \hat{A}] = \langle X | \hat{A} | X \rangle, \quad (3)$$

which is known as the Husimi representation of the operator. The covariant and contravariant symbols are not identical in the coherent states representation. Replacing (2) in (3) we find that they are related by the following expression

$$\begin{aligned}A_H(X) &= \frac{1}{2\pi\hbar} \int dX' \tilde{A}_H(X') \text{Tr} [\hat{\rho}_X \hat{\rho}_{X'}] \\ &= \int dX' \tilde{A}_H(X') G_{2\hbar}(X - X').\end{aligned}\quad (4)$$

It is clear that the contravariant symbol $\tilde{A}_H(X)$ contains all the information on the operator \hat{A} since it performs a decomposition on a complete basis. However, for the covariant symbol $A_H(X)$, the Gaussian smoothing of the contravariant one (see (4)) could produce some loss of information. It is only the special analytical properties of $A_H(X)$ [18] that ensures that this symbol contains all the information on \hat{A} .

It is also possible to obtain the covariant symbol $A_H(X)$ from the Weyl symbol $A_W(x)$. For this purpose, we need to use the Wigner function of a coherent state $|X\rangle$ that takes the form (see [15])

$$\rho_X(x) = \text{Tr} [\hat{R}_x \hat{\rho}_X] = 2\hbar\pi G_\hbar(X - x).$$

Then, the coherent state projectors can be written in terms of reflection operators as follows

$$\hat{\rho}_X = \frac{1}{2\pi\hbar} \int dx \hat{R}_x \rho_X(x) = \int dx \hat{R}_x G_\hbar(X - x), \quad (5)$$

that is, as a Gaussian smoothing on an area of size \hbar . Finally, we obtain $A_H(X) = \text{Tr} [\hat{\rho}_X \hat{A}] = \int dx G_\hbar(X - x) A_W(x)$, showing that the Husimi representation is a

Gaussian smoothing of the Wigner function on an area of size \hbar .

Let us now define, analogously to (5), a new set of operators \hat{O}_X^σ , that we will call Smoothed Reflection (SR) operators. This new set is obtained as a Gaussian smoothing from the reflection operators on an area of size \hbar^σ

$$\hat{O}_X^\sigma = \int dx \hat{R}_x G_{\hbar^\sigma}(X - x).$$

For $\sigma = 1$ we recover the coherent state projectors $\hat{O}_X^1 = \hat{\rho}_X$ (see (5)), while for $\sigma \rightarrow \infty$ the Gaussian distribution leads to a delta distribution and $\hat{O}_X^\sigma \rightarrow \hat{R}_x$. Moreover using (1), the set of SR operators results a decomposition of the unity

$$\frac{1}{2\pi\hbar} \int \hat{O}_X^\sigma dX = \hat{1},$$

and the trace of two SR operators leads to

$$\begin{aligned} \text{Tr} \left[\hat{O}_{X_1}^\sigma \hat{O}_{X_2}^\sigma \right] &= \int dx_1 dx_2 \text{Tr} \left[\hat{R}_{x_1} \hat{R}_{x_2} \right] \\ &\quad \times G_{\hbar^\sigma}(X_1 - x_1) G_{\hbar^\sigma}(X_2 - x_2). \end{aligned}$$

Using the orthogonality relation (1) in order to integrate the x_2 variable, and performing the resulting Gaussian integral with the following easily verifiable property

$$G_{a_1+a_2}(X - X') = \int dx G_{a_1}(X - x) G_{a_2}(x - X'), \quad (6)$$

there results

$$\text{Tr} \left[\hat{O}_{X_1}^\sigma \hat{O}_{X_2}^\sigma \right] = 2\pi\hbar G_{2\hbar^\sigma}(X_1 - X_2). \quad (7)$$

As for the coherent state representation, the decomposition of an operator \hat{A} in terms of the set of operators \hat{O}_X^σ defines the contravariant SR symbol $\tilde{A}_\sigma(X)$

$$\hat{A} = \frac{1}{2\pi\hbar} \int dX \tilde{A}_\sigma(X) \hat{O}_X^\sigma.$$

On the other hand, the trace operation defines the covariant symbol, which can be obtained from the Weyl representation as a Gaussian smoothing on an area of size \hbar^σ

$$A_\sigma(X) = \text{Tr} \left[\hat{O}_X^\sigma \hat{A} \right] = \int dx G_{\hbar^\sigma}(X - x) A_W(x).$$

Using (7), the relation between covariant and contravariant symbols in the SR representation results

$$\begin{aligned} A_\sigma(X) &= \frac{1}{2\pi\hbar} \int dX' \tilde{A}_\sigma(X') \text{Tr} \left[\hat{O}_X^\sigma \hat{O}_{X'}^\sigma \right] \\ &= \int dX' \tilde{A}_\sigma(X') G_{2\hbar^\sigma}(X - X'). \end{aligned}$$

Also, knowing the covariant SR symbol for $\hbar^\sigma < \hbar$, the Husimi covariant symbol is obtained as follows

$$\begin{aligned} A_H(X) &= \int dx G_{\hbar}(X - x) A_W(x) \\ &= \int dX' G_{\hbar-\hbar^\sigma}(X - X') A_\sigma(X'), \end{aligned} \quad (8)$$

where in the last equality we have used (6).

The completeness of the covariant SR symbol is obtained through its ability to recover the Husimi symbol (8). Although a smoothing of the Wigner symbols could imply a loss of information, the special analytical properties of the Husimi representation, as we already mentioned, contains all the information on the operator. Relation (8) implies that the Husimi symbol can be obtained from the SR covariant symbol by performing a Gaussian smoothing on a phase space region of size $\hbar - \hbar^\sigma$, when $\hbar^\sigma \leq \hbar$. This shows that the covariant SR symbol contains all the information on the operator. Nevertheless, for values of σ such that $\hbar^\sigma > \hbar$, we cannot obtain a relation like (8), so in this case the completeness of the SR symbol is not guaranteed.

In the original paper by Cahill and Glauber [9] the smoothing of the Wigner function was labeled by the complex number s . In this paper, instead, we have used \hbar^σ to explicitly show the broadening of the Wigner function in terms of the Planck constant. In order to translate both formalisms, our scheme is equivalent to take a $\Im(s) = 0$ and $\Re(s) = -\hbar^{\sigma-1}$.

In summary, we have described the representation of quantum mechanics associated with a sub-Planck smearing of the Wigner function in the formalism of reflection operators in phase space. In what follows, we will illustrate the usefulness of this representation for the study of the semiclassical limit of quantum mechanics. As we have already mentioned, the Wigner or Husimi representations suffers for different pathologies in order to correctly resolve semiclassical structures. The Wigner function presents quantum interference between distant localized objects [5], while the Husimi function washes out the interference but only resolves objects on an area of size \hbar hiding lower scale semiclassical structures [8]. So it is natural to think that a compromise solution where a smoothing of the Wigner function is performed, in an area of size lower than \hbar , would be more appropriated.

One of the most important problems in quantum chaos is to understand how the classical orbits and their stability structure let imprints in quantum mechanics. In particular, the scarring phenomenon appears when the probability density is enhanced along unstable periodic orbits.

In order to show the usefulness of the smoothed Wigner function to resolve semiclassical structures, we apply the intermediate smoothing representation to uncover hyperbolic structures present in the eigenfunctions of the Bunimovich stadium billiard. This system is fully chaotic and has great theoretical and experimental relevance [19–21]. It consists of a free particle inside a 2-dimensional planar region whose boundary is shown in Figure 1.

In Figure 1a we show the coordinate representation of an excited state $|\psi\rangle$ which presents an important scarring on the bowtie orbit and contribution of an orbit near the bouncing ball region. Both orbits are shown in Figure 1b.

Figures 2a–2d show the smoothed reflection representation of the density operator $\hat{\rho}^\psi = |\psi\rangle\langle\psi|$ in Birkhoff [22]

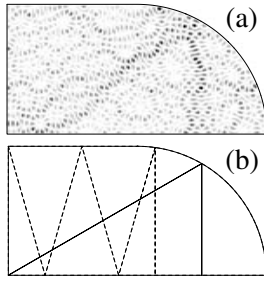


Fig. 1. The desymmetrized Bunimovich stadium billiard, with radius r taken equal to unity and enclosed area $1 + \pi/4$. In panel (a) the linear density plot in configuration space (position representation) of $|\psi\rangle$ is shown for the state with wave number $k = 100.255$. While in panel (b) two relevant orbits are displayed, the bowtie orbit in full line and an orbit near the bouncing ball region in dashed lines.

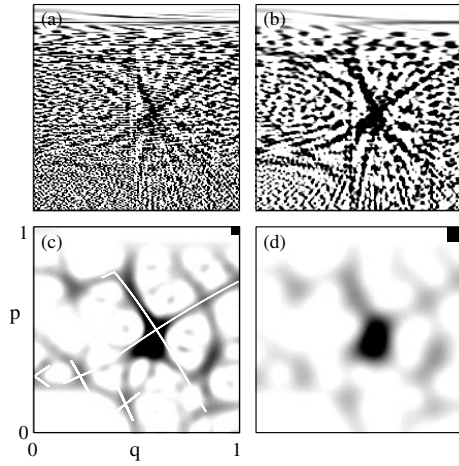


Fig. 2. Phase space representations $\rho_\sigma^\psi(p, q)$ of the state with wave number $k = 100.255$ for the desymmetrized Bunimovich stadium billiard. The parameter $\sigma = 2.25, 1.75, 1.165$ and 1 for panels (a), (b), (c) and (d). The plotting convention is that for each panel a linear gray scale is used such that the maximum of the distribution is denoted in black, while white color is used for the minimum. In the up right corner of each panel a black square of size \hbar^σ is drawn. This square is too small to be noted in panels (a) and (b). In panel (c) the full white lines represents the stable and unstable manifolds for the bowtie orbit and for the orbit near the bouncing ball region described in Figure 1b.

coordinates, with

$$\begin{aligned} \rho_\sigma^\psi(p, q) &= \text{Tr} \left[\hat{O}_X^\sigma \hat{\rho}^\psi \right] = \text{Tr} \left[\hat{O}_X^\sigma |\psi\rangle \langle \psi| \right] \\ &= \int dx G_{\hbar^\sigma}(X - x) \rho_W^\psi(x), \end{aligned} \quad (9)$$

and $\sigma = 2.25, 1.75, 1.165$ and 1 respectively. The plotting convention is that for each panel a linear gray scale is used such that the maximum of the distribution is denoted in black, while white color is used for the minimum. It has to be noted that, the distributions plotted takes positive and negative values, except for Figure 2d that describes the positively defined Husimi distribution. As it was mentioned before, the finest structures of the Wigner function are

of size \hbar^2 [5], so $\rho_\sigma^\psi(p, q)$ practically results the Wigner function for $\sigma = 2.25$ (see Fig. 2a).

A chaotic eigenfunction is semiclassically constructed by the sum of contributions of all periodic orbits with period up to around the Ehrenfest time [23]. Moreover, the Wigner function of each contribution consists of long range hyperbolic fringes asymptotic to the stable and unstable manifolds [8]. Nevertheless, it is difficult to observe these hyperbolic patterns in the Wigner function of a chaotic eigenfunction because the characteristic fringe patterns highly interfere. For this reason, the hyperbolic structure of individual periodic orbits is poorly seen in Figure 2a. On the other hand, the Husimi distribution corresponding to $\sigma = 1$ washes out localization on the stable and unstable manifolds of the bowtie orbit as it is shown in Figure 2d. Finally, for intermediate values of σ (Figs. 2b and 2c) the interference is dampened, and regions of high intensity of the distribution locate along the manifolds. Indeed in Figure 2c it is also possible to distinguish regions of high intensity located along the hyperbolic structure of the orbit near the bouncing ball region previously shown in Figure 1b.

The previous mentioned discrepancies among different smoothness result essential for studying the scar phenomenon. It was shown recently [24] that by using hyperbolic structures in order to measure localization on short periodic orbits, the scar phenomenon survive the semiclassical limit. This means that the sum of scarred intensities of a generic chaotic eigenfunction takes in this limit a non null value which only depends on classical invariants of the system. On the contrary, by using wave packets in the transverse direction to the motion (for instance, the coherent states used in the Husimi distribution), the sum of scarred intensities tends to zero in the semiclassical limit. The consequences of these results for our particular example should be interpreted as follows. In Figures 2c and 2d we observe that the maxima of the distributions are located near fixed points associated to periodic orbits. Such correspondence should survive the semiclassical limit for an adequate intermediate distribution that washes out the long range fringes of the Wigner but which any way displays the hyperbolic structure along the manifolds. On the other hand, the maxima of the Husimi distribution should be of pure quantum nature in the semiclassical limit, and we do not expect any correspondence with classical objects.

As another example of the potential use of these intermediate representations, we mention that the same kind of smoothing is shown to occurs in the context of decoherence [25]. In that case, the smoothing of the Wigner function is a natural consequence of time evolution because of the presence of decoherence. As a matter of fact, the time decohered Wigner function is a Gaussian smoothing of the original one, so that the quantum interference disappear and the classical structures emerge. While, in [26] the smoothed reflection operators are used to generate decoherence at each step of the quantum map.

In conclusion, we have described a one parameter family of phase space representations of quantum mechanics

that has the Wigner and Husimi representations as extremes cases. But also it is able to explore intermediate resolutions for the purpose of enhancing the quantal resolution of the Husimi function or to dampen interference effects of the Wigner representation. We have shown that this is a good representation of quantum mechanics in the sense that it contains all the information of the states, and we performed its description in the modern language of smoothed reflection operators in phase space. Also, we have shown the usefulness of this representation to resolve semiclassical structures in quantum mechanics. In particular it permits to better visualize the scarring phenomenon, distinguishing periodic points with its stable and unstable manifolds. This is particularly useful for futures studies in a better understanding of the semiclassical limit of quantum mechanics.

We would like to thanks Marcos Saraceno and Alfredo M. Ozorio de Almeida for fruitful discussions and suggestions. We acknowledge financial support from Conicet.

References

1. M.C. Gutzwiller, *Chaos in Classical and Quantum Mechanics* (Springer-Verlag, NY, 1990)
2. N.L. Balazs, B.K. Jennings, Phys. Rep. **104**, 348 (1984)
3. M.V. Berry, M. Tabor, J. Phys. A: Math. Gen. **10**, 371 (1977)
4. J.M. Tualle, A. Voros, Chaos Solitons, Fractals **5**, 1085 (1995)
5. W.H. Zurek, Nature **412**, 712 (2001)
6. Z.P. Karkuszewski, C. Jarzynski, W.H. Zurek, Phys. Rev. Lett. **89**, 170405 (2002)
7. D.A. Wisniacki, Phys. Rev. E **67**, 016205 (2003)
8. A.M.F. Rivas, A.M. Ozorio de Almeida, Nonlinearity **15**, 681 (2002)
9. K.E. Cahill, R.J. Glauber, Phys. Rev. **177**, 1856 (1969); Phys. Rev. **177**, 1969 (1969)
10. J. Fiurášek, Phys. Rev. A **62**, 013822 (2000)
11. E.J. Heller, Phys. Rev. Lett. **53**, 1515 (1984)
12. L. Kaplan, Nonlinearity **12**, R1 (1999)
13. A.M.F. Rivas, in preparation
14. For example in the case of a particle of mass m moving with kinetic energy E in a stadium billiard, the perimeter of the boundary is the characteristic length when we use Birkhoff coordinates [22], while the characteristic momentum is given by $\sqrt{2mE}$
15. A.M. Ozorio de Almeida, Phys. Rep. **295**, 265 (1998)
16. A. Perelomov, *Generalized Coherent States and their Applications* (Springer, New York, 1986)
17. F.A. Berezin, Sov. Phys. Usp. **132**, 497 (1980)
18. V. Bargmann, *Analytic methods in Mathematical Physics* (Gordon and Breach, New York, 1970), Vol. 74
19. L.A. Bunimovich, Funct. Anal. Appl. **8**, 254 (1974)
20. A.G. Huibers et al., Phys. Rev. Lett. **83**, 5090 (1999)
21. M. Switkes, C.M. Marcus, K. Campman, A.C. Gossard, Science **283**, 1905 (1999)
22. Once the flow is studied through the collision map on the boundary. The place where the collision occurs and the incident angle are canonically conjugate coordinates called the Birkhoff coordinates
23. E.G. Vergini, J. Phys. A: Math. Gen. **33**, 4709 (2000)
24. E.G. Vergini, J. Phys. A: Math. Gen. **37**, 6507 (2004)
25. O. Brodier, A.M. Ozorio de Almeida, Phys. Rev. E **69**, 016204 (2004)
26. I. García-Mata, M. Saraceno, M.E. Spina, Phys. Rev. Lett. **91**, 064101 (2003)